Cellular Physiology and Biochemistry

Cell Physiol Biochem 2018;45:783-794
DOI: 10.1159/000487170
Published online: February 06, 2018
Accepted: Novermber 29, 2017

Original Paper

Functional Implications of Cross-Linked Actin Networks in Trabecular Meshwork Cells

Laura Duffy Steven O'Reilly

Faculty of Health and Life Sciences, Northumbria University, Newcastle Upon Tyne, Tyne and Wear, United Kingdom

Key Words
Trabecular meshwork • Actin • Cross-linked actin • Phalloidin • Geodesic domes

Abstract
Background/Aims: The Trabecular meshwork (TM) is the tissue responsible for outflow resistance and therefore intraocular pressure. TM cells contain a contractile apparatus that is composed of actin stress fibres which run parallel to the axis of the cell and are responsible for facilitating contraction. Cross-Linked Actin Networks (CLANs) are polygonal arrangements of actin that form a geodesic network found predominantly in TM cells both in situ and *in vitro*. The aim of this work is to determine the functional significance of CLANs in TM cells and to assess the effect of mechanical stretch stimulation on the induction (or not) of CLANs. ***Methods:*** We used collagen gel contraction models to demonstrate functional impairment of cells when induced to express CLANs in situ. Cyclic mechanical stretch was used to stimulate cells and measure CLANs ***Results:*** CLANs inhibited contraction and cyclic mechanical stretch induced CLANs. Furthermore, we also demonstrated that using shape alone we could predict the appearance of CLANs using a simple light microscopy technique. ***Conclusion:*** Taken together we have now shown, for the first time, a functional deficit In TM cells with CLANs Furthermore that shape alone can predict the appearance of CLAN containing cells. CLANs can now be linked to a functional effect and may underlie the appearance of CLANs with the pathology of primary open angle glaucoma (POAG).

Introduction

The evolutionary conversed actin cytoskeleton is essential in mediating many functions of the cell including locomotion, division, contraction and phagocytosis. The common patterns of actin microfilament arrangement within eukaryotic cells are diffuse, F-actin arrangements and parallel microfilaments which are tightly bundled together to form stress fibres and cortical actin [1]. However, there is another type of actin arrangement of F-actin

Steven O'Reilly

Faculty of Health and Life Sciences, Northumbria University,
Newcastle Upon Tyne Tyne and Wear (United Kingdom)
Tel.+441912224780, E-Mail steven.oreilly@northumbria.ac.uk

found within cells. This is a dome like arrangement of F-actin microfilaments made up of units of polygonal actin networks [2]. Lazarides first described these polygonal actin arrays in culture and found that they appear after freshly plated out from trypsinisation and then disappeared as the cultures became established [2]. Cross-Linked Actin Networks (CLANs) appear very similar to these actin structures, they contain polygonal actin arrangements, with a central hub and radiating vertices, often in patterns of five or six and are found in confluent cultures of trabecular meshwork cells (TM) [3-5].

TM cells are specialised cells that line the trabecula in the outflow tract of the eye and through here aqueous humour drains. The aqueous humour drains through the TM, a multi-layered tissue in the iridocorneal angle of the eye. These CLANs appear to have architectural similarities to the transient structures seen in other cells [2, 6, 7]. An important feature of CLANs is that they are induced upon exposure to various steroids including dexamethasone (DEX) and not induced in a variety of other cell types tested [3]. Steroid-induced ocular hypertension is thought to result through changes to the ocular outflow pathway mediated through steroid-induced alterations in TM cell function including alterations in phagocytosis and cell migration. The biggest risk factor for primary open angle glaucoma is raised intraocular pressure (IOP) which can be raised with steroid use. The functional significance of CLANs are unknown however, atomic force microscopy appears to suggest they impart a structural rigidity to the cells [8, 9]. Such structural rigidity may impact on the vital functions of the cells and it is of note that CLANs are found with higher frequency in glaucoma donors [3]. Whilst CLANs have been found in TM both *in vitro* and in ex vivo tissues, excluding they are an artefact, it remains to be determined if they have any functional roles (if any). The aim of this study was to determine the functional effects of CLANs using contraction, viability and mechanical stretch and also to determine if CLAN identification was associated with a particular cell phenotype.

Materials and Methods

Isolation of Bovine TM cells

Bovine TM (BTM) cells were isolated from bovine eyes sourced from a local abattoir from 10-12 individual donors and were washed in antibiotic solution (Penicillin, Sigma, UK). Tusing the method described by Wade et al. [10]. Cells were then cultured in DMEM (Sigma, UK) supplemented with 10% (vol/vol) Foetal Calf Serum (FCS) which was previously heat inactivated.

Preparation of 2 and 3D collagen matrices

The method has been described previously and was used here [11], the source of the collagen is rat tail collagen type I (Gibco, UK) and the final concentration was 1.5 mg/ml and was solidified by slowly raising the pH with 1M NaOH. Gel contraction studies were performed in 24-well plates. 2D gels were formed by setting the collagen matrix cell-free and subsequently placing the cells upon this collagen matrices (2D). 3D cultured cells were placed within the collagen gels, so that they are dispersed within the matrix (3D).

After 10 minutes the matrices were overlaid with complete medium with or without DEX 10^{-7}M, detached from the base using a sterile pipette tip and floated in the well plates. At set time points the matrices were measured using Image J software (NIH, US) and expressed as area.

F-actin staining of cells within collagen matrices

Collagen matrices were removed from the wells and fixed in 10% Neutral Buffered Formalin (10% NBF), permeabilised with 0.5% Triton-X 100 (Sigma, UK) and then stained with Phalloidin Alexa-488 for 2 hours (for actin visualisation), washed 3 times with Tris buffered saline (TBS) solution, and mounted on a slide with mounting media (Vectashield, UK). Images were taken using a laser scanning confocal microscope. CLANs were identified using our criteria of three triangulated arrangements of actin. Random areas were chosen to identify CLAN-containing cells. Due to the limitations of the microscope and the auto fluorescence of the collagen matrix a full quantification of CLANs could not be performed.

Cyclic Mechanical stretch

Cells were grown on flexcell plates then treated with DEX for 14 days. After 14 days in culture post confluence with either control or Dex 10^{-7}M the plates were placed onto the Flexcell™ FX5000 system (Flexcell, USA) and received cyclic mechanical stretch of 10% elongation 1Hz for 12 hours. This regime of stretch was chosen to replicate the pulsatile mechanical forces found *in vivo* [12, 13]. The Flexcell plates are composed of silicone to facilitate the stretching and to help adherence of cells to the silicone they are coated with fibronectin. Media was then removed and stored at - 80°C, for subsequent analysis. Cells were fixed and stained for F-actin as described above.

TGF-β2/IL-6 quantitation

The conditioned medium from the above experiment was used in IL-6 and TGF-β2 ELISAs from R&D systems (UK) following the manufactures protocol which included incubating the conditioned media within the antibody coated well and then using a detection antibody that is HRP-conjugated and then developing and reading on a Tecan plate reader. These are validated ELISAs from a commercial supplier.

H_20_2 measurement

After the stretch regime cell media was measured for H_20_2 levels using Amplex Red (Invitrogen, UK) which is a highly stable and sensitive probe for H_20_2.

Western Blotting

After 10% cyclic mechanic stretch, cells were lysed in RIPA buffer containing a protease inhibitor cocktail. A 10% SDS-PAGE was carried out using 30 μg of total protein cell lysates. The SDS-PAGE gel was then transferred onto PVDF membrane using wet transfer for 1 hour in transfer buffer. The membranes were blotted with anti-SuperOxide Dismutase-1 (SOD1) antibodies (Santa Cruz, UK), and re-probed for GAPDH as a loading control (Santa Cruz, UK). HRP-conjugated secondary antibody was used for detection with Enhanced Chemiluminecent (ECL) substrate (Biorad, UK) and developed using detection film.

qRT-PCR

After cyclic mechanical stretch, cells were lysed in TRIzol reagent (Invitrogen, UK) and RNA was isolated following the manufacturers protocol. 1μg of RNA was reverse transcribed to cDNA using superscript (Invitrogen) after DNAse treatment qPCR was performed using 0.25mM primers for Connective Tissue Growth Factor (CTGF), sense 5′-GAAAGGCAAAAAGTGCATCC-3′, antisense 5′-CTTGTGCCACTGAAATCACG-3′, Matrix Mettaloproteinase-2 (MMP-2) sense 5′-GGGGAGATTCCCACTTTGAT-3′, antisense 5′-TGCAGTCGGTGTACTCCTTG-3′ 18S, sense 5′-GTGGAGCGATTTGTCTGGTT-3′, antisense 5′-CGCTGAGCCAGTCAGTGTAG-3′ using SYBR green (Sigma, UK). 18s was used as the housekeeping gene and data was calculated as fold change using the 2delta delta Ct method. All amplicons were verified with a melt curve and agarose gel electrophoresis was performed to confirm a single amplicon of the correct size.

CLANS and morphology

BTM cells were seeded at a cell density of $1x10^4$ cells, cells were then treated with DEX 10^{-7}M, TGF-β2 2ng/ml or decorin 25μg/ml for seven days. On day 7, the cells were fixed and stained, as above, and analysed using fluorescence microscopy. Selection was always done in fluorescence mode and then the exact same image was taken in phase contrast mode. Selection of fields was always done in fluorescence mode and based on the presence of a cell with a CLAN or a cell with clear stress fibres only. The cells were categorised as belonging to three distinct shapes epitheloid (round), spindle (an elongated polarised form) and kite shaped cells (polygonal).

Circularity was calculated in after tracing the perimeter of the cell. The circularity is calculated from the formula: $4\pi(\text{area}/\text{perimeter}^2)$.

Time lapse imaging of BTM cells

Cells were seeded onto glass bottomed Iwaki six-well plates (Iwaki, Japan) and then treated with DEX 10^{-7}M, TGF-β2 or decorin 25 μg/ml for 7 days after which the plates were placed into a microscope holder inside an incubator that controlled the temperature (37°C) and live phase contrast images were recorded over 20 hour period using a Zeiss microscope with a X 20 objective. At the end of the phase contrast filming

period the cells were fixed in 10% NBF and stained as above. After staining the cells were analysed on the basis of clear fluorescent staining and their appearance was easy to classify. We then looked at the three classifications of cell shape and followed their life history in the culture. An arbitrary scale for locomotion of the cells was employed where M* cells moved at 4μm/hour or less, M** reached up to 12μm/hour, whereas above that M*** cells were faster still and some could reach a movement rate of 25μm/hour for short periods, M**** is for cells that moved extremely quickly in the culture. Speed was calculated by distance and time.

Results

Collagen contraction models

Collagen contraction models were used to determine cellular contraction of the cells in both a 3D and 2D environment and are an accepted model of cellular contraction [11]. Employing 3D collagen matrices, where the cells are embedded within the collagen, it was shown that only at day five was there any significant difference in contraction between untreated and DEX exposed cultures (Fig. 1A). However, in the 2D collagen matrices it was clear that at day 5 the DEX-incubated matrices had over 50% inhibition of contraction compared to control and by day 7 over 70% inhibition of contraction of the collagen matrices had occurred both P=<0.05 (Student's t- test) (see Fig. 1B).

Contraction-inhibited matrices contain CLANs

A logical next step was to demonstrate the presence of CLANs within the collagen matrices. After cessation of the experiment the matrices were fixed and stained to visualise F-actin with phalloidin. Fig. 1C shows a confocal image of a CLAN on a contraction-inhibited

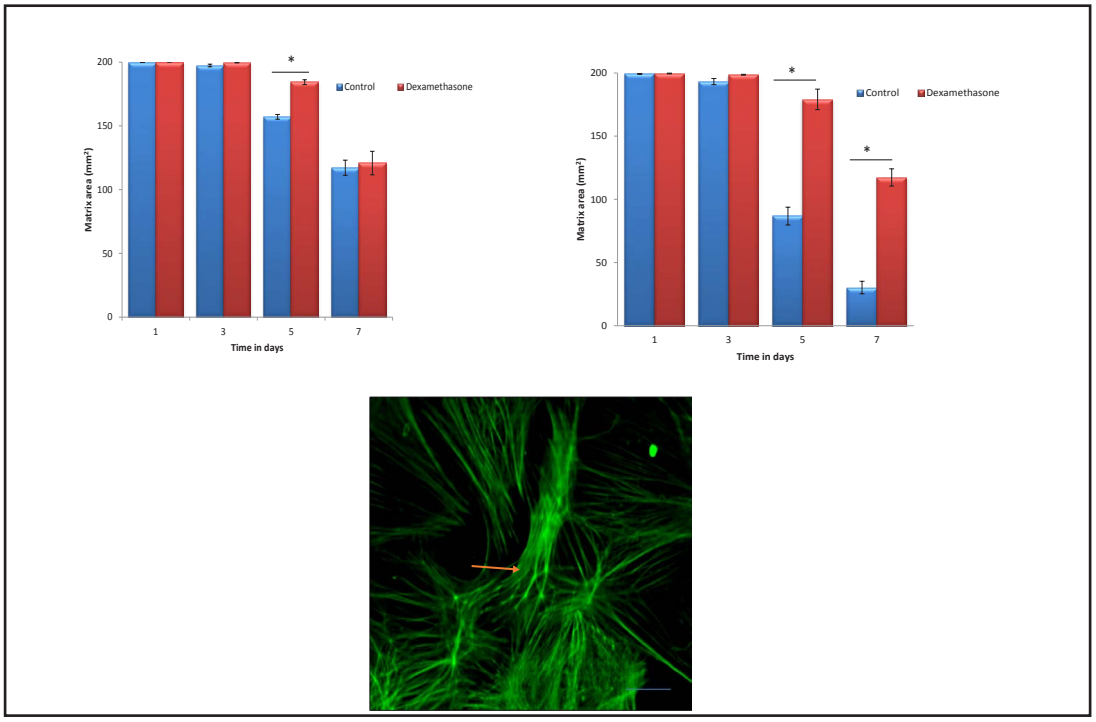

Fig. 1. Collagen contraction is attenuated by CLANs: 1A). 3D Collagen gels were populated with BTM cells and cultured for up to seven days with or without the addition of DEX (10^{-7}M) and the area was quantified. Data is the mean and SEM. 1B). 2D collagen gels were populated with BTM cells with or without the addition of DEX (10^{-7}M) for up to seven days, significant differences are apparent between DEX-treated and control populated matrices. Data is the mean and SEM. *= P=<0.05 Students t test. 1C) CLAN-containing 2D DEX-treated collagen gel fixed and stained with phalloidin Alexa flour-488 and imaged using confocal microscopy. Arrow indicates CLAN. Scale bar= 20μm.

2D matrix stained with phalloidin-FITC. The 'hub' points for CLANs are clearly evident (shown in Fig. 1C). The left hand side of the image shows another CLAN. The prominent pattern in the control matrices that were not exposed to DEX was that of stress fibres. Semi-quantitative analysis revealed more CLANs in DEX-treated cultures than in control.

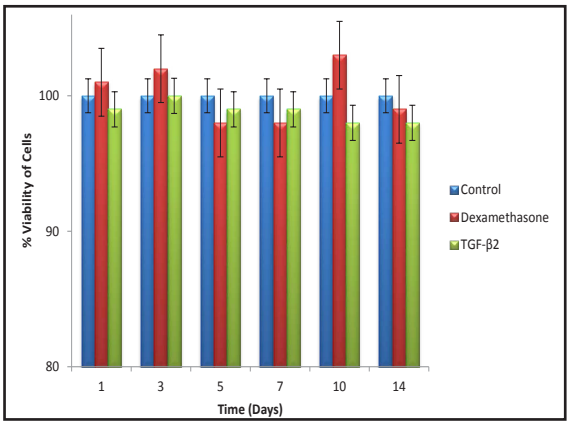

Fig. 2. No decrease in cell viability with CLAN inducers. % viability of BTM cells treated with CLAN inducing agents and exposed to trypan blue at specific time periods. Data is the mean and SD n=10.

To confirm the contraction inhibition was not simply due to cell death induced by DEX, It was important to evaluate the effect of DEX/CLANs on cell survival, as CLANs could be associated with cell death; therefore we undertook assays to assess the effect of the glucocorticoid on cellular death. General morphological characterisation of cells after treatment, using phase contrast microscopy did not reveal any gross changes associated with cell death. Trypan blue exclusion was initially used to determine any changes in cell death. Viability was always over 97% in the culture conditions both treated and untreated (Fig. 2). Furthermore, we used the MTT assay to evaluate cell viability and there were no significant differences between control, DEX or TGF-β2 cultures (data not shown).

Physiological stretch leads to CLANs

We sought to determine if cyclic radial mechanical stretching of BTM cells results in induction of CLANs. Using a Flexcell™ stretching equipment cells were subjected to 10% mechanical strain (1 cycle/1sec) for a period of 12 hours. This stretch regime was chosen to replicate the pulsatile biomechanical forces to which the normal TM is exposed *in vivo* and 10% mechanical stretch is suggested to be physiological [12, 13]. Investigations determined full cell attachment, with cells being well spread (Fig. 3A). Results of our stretch regime on CLAN incidence reveals that stretch increased CLANs to 40.5% compared to 20% grown on the same substrate but not exposed to cyclic stretch regime, representing a 100% increase in CLAN incidence compared to un-stretched control (P=<0.01). BTM exposed to stretch and pre-incubated with DEX for 14 days resulted in 53% CLANs compared to control this is significantly different (P=<0.01; ANOVA). Cells that were incubated with DEX and were not subjected to stretch CLAN incidence was 49% CLANs in equivalent cultures that did not receive cyclic stretch. (Fig. 3B).

Phenotypically these CLANs were similar to DeEX, TGF-β2 and decorin produced CLANs. The conspicuous dominant pattern of actin in the control treated and un-stretched membrane was that of stress fibres. However, in this un-stretched culture CLANs were clearly evident with around 20% of cells containing CLANs comparing this to our usual basal level of CLANs incubated on normal tissue culture plastics (and no matrix substrate) of 6.2% CLANs means there is a large change in CLAN numbers, therefore indicating that extracellular matrix may play a facilitative role in formation of CLANs, at least *in vitro* [14]. Such CLANs were clearly present after only 12 hours of stretch suggesting generation of CLANs can occur relatively quickly. Analysis of the cells revealed no damage [15] or increased H_20_2 levels (Fig. 3C) which suggests that the cells are not under extensive stress. Immunoblotting revealed no difference in SOD1 levels after stretch either (Fig. 3D).

TGF-β2 and IL-6 is upregulated in response to cyclic stretch

As TGF-β2 is a known inducer of CLANs *in vitro* we decided to measure the levels of this mediator. This was acid activated to liberate the 'active' form of TGF-β2. Secreted TGF-β2

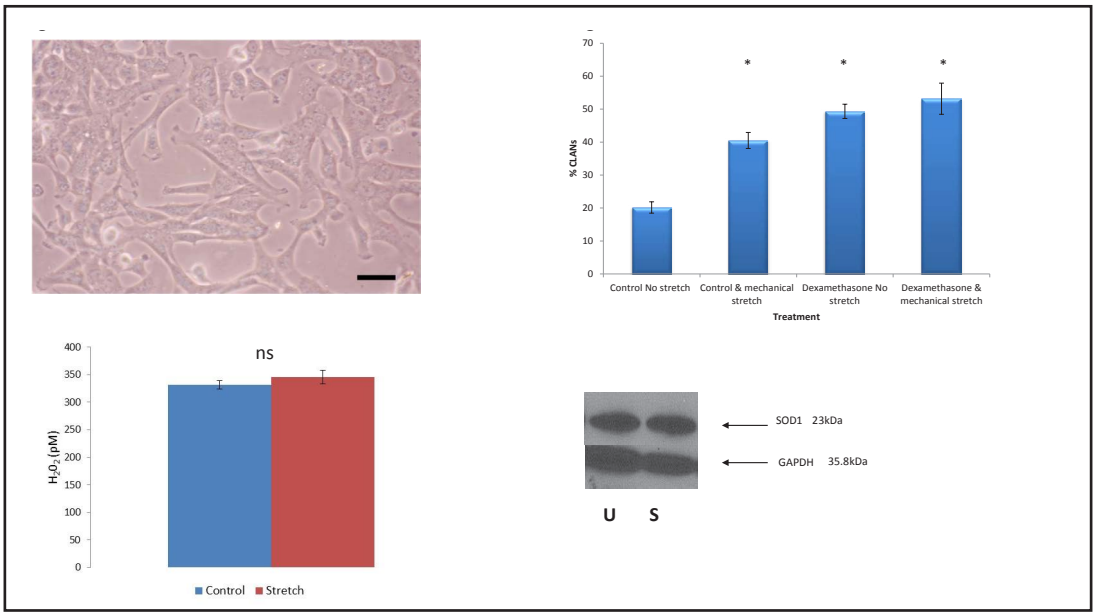

Fig. 3. Cyclic mechanical stress in BTM cells induces CLANs. A). Representative phase contrast micrograph of BTM cells on the fibronectin-coated silicone membrane used for stretching the cells. B). BTM cells percentage CLAN-positive cells. BTM cells were subjected to 10% cyclic mechanical strain using a Flexcell system after being stimulated with or without DEX (10^{-7}M) for 14 days after which cells were fixed and stained for actin and CLANs positive cells were quantified. Data is the mean and SD n=5. C). No increase in H_20_2 production in media after mechanical stretch. After cyclic mechanical stretch medium was removed and measured for H_20_2 by Amplex Red. Data is the mean and SD n=5. (D). Representative western blot of SOD1 after cyclic mechanical stretch cells were lysed and blotted with anti-SOD1 antibodies. GAPDH was re-probed as loading control. U= unstretched, S= stretched n=5.

was found to be 500pg/ml in control cultures not exposed to mechanical stretch, however mechanical stretch led to an upregulation of TGF-β2 expression in culture medium (657pg/ml) which was highly statistically significant (*P*=<0.05 ANOVA). In DEX stimulated cultures the TGF- β2 levels were 601pg/ml and DEX-exposed and stretched levels were 556pg/ml. Incubation with DEX and mechanical stretch resulted in less TGF-β2 secretion than DEX alone; however, this was only a small decrease and clearly not significant as Fig. 4A demonstrates.

Soluble IL-6 was below the limit of detection in the ELISA for control un-stretched, however after being subjected to mechanical stretch IL-6 levels were 2488pg/ml and 4351pg/ml with DEX treatment alone and 5842pg/ml with mechanical stretch and DEX treatment (Fig. 4B). Using RT-PCR arrays we found that compared to control untreated IL-6 mRNA was 2.5 fold elevated with both DEX and TGF-β2 exposure (data not shown). Furthermore, Connective Tissue Growth Factor (CTGF) which is a known target gene of TGF-β, was also significantly elevated compared to un-stretched cultures *P*=<0.05 Student's t test (Fig. 4C). However, we seen no difference in MMP-2 mRNA expression.

CLAN containing BTM cells display an altered morphological phenotype

It was evident that all our stimulants of CLAN formation caused some level of shape change in the cultures exposed to the CLAN stimuli. A question arose as to whether BTM cells containing CLANs were at all different in appearance from those cells rich in stress fibres and whether there was any relationship to the cell-shape changes produced by our CLAN induction agents. Selection of fields was always done in fluorescence mode and based on the presence of a cell with a CLAN or a cell with clear stress fibres only. Almost invariably in BTM primary cultures, even when comparing those established from different eyes and at different passage number, three distinctive cell appearances were identified by

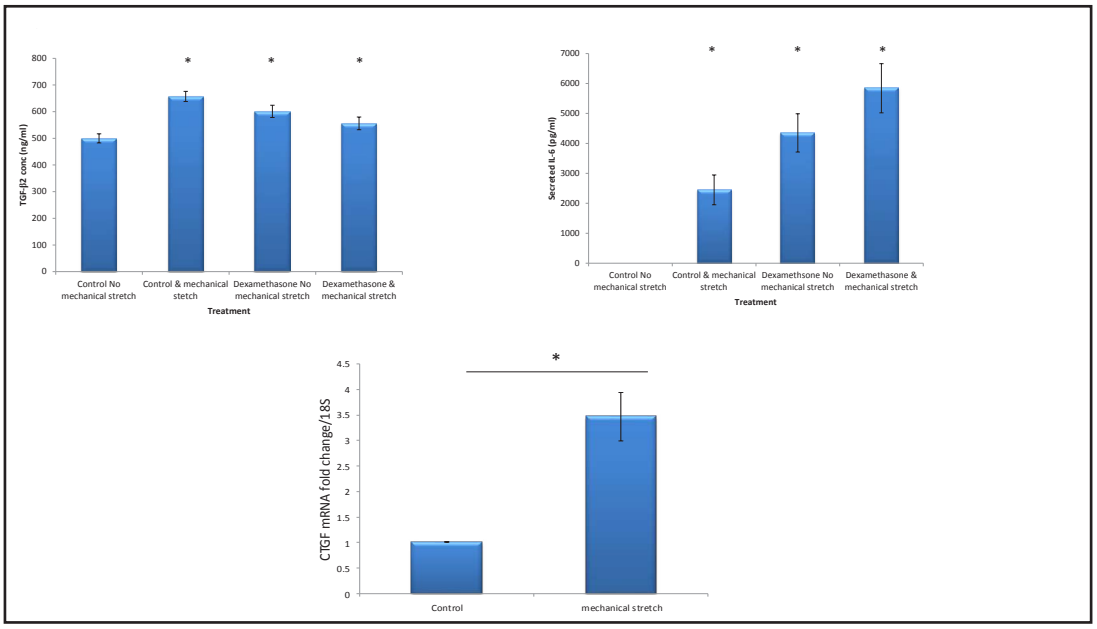

Fig. 4. TGF-β2 induction by cyclic mechanical stress in BTM cells. A). TGF-β2 levels were quantified by ELISA after cyclic mechanical stretch with or without DEX (10^{-7}M) stimulation for 14 days after acid activation of latent TGF-β2. *= P=<0.05 compared to control un-stretched. N=5. B). IL-6 levels were quantified by ELISA after cyclic mechanical stretch with or without DEX (10^{-7}M). Data is the mean and SD n=5. C). qRT-PCR was performed for CTGF after mechanical stretch and normalised to the internal housekeeping gene 18S. Data is mean fold change and SD n=5 *=P=<0.05 Students t test.

phase contrast microscopy that we called spindle, epithelioid and kite shaped cells. Fig. 5A illustrates the idealised cells. After treatment with DEX, TGF-β2 and decorin the incidence of spindle (40%) and epithelioid (40%) were much the same but each was twice as abundant as kite shaped cells (20%).

Fig. 5B illustrates that CLAN containing cells have a different phenotype to none-CLAN-containing cells. BTM cells that are kite shaped are just as likely to have stress fibres as they are to have CLANs, so neither actin arrangement is a predictor of this cell shape. However, BTM cells containing stress fibres tend predominantly to be spindle shaped whereas those cells with CLANs tend primarily to be epithelioid (Fig. 5C). Intriguingly the pattern is repeated remarkably consistently irrespective of what CLAN inducing agent is employed. As might be expected from the results of our classification findings, image analysis showed that CLAN-containing cells were significantly more rounded (0.63) (a circularity of 1 indicates a perfect sphere) than stress-fibre only containing cells for each of the CLAN inducing agents used in this part of the investigation (*P*=<0.01, Student's t test) Fig. 6. Therefore, this added a level of support to the concept that CLAN-containing cells tend to be rounded. Indeed another parameter measured was total area of the BTM cell and this was found to be increased in CLAN containing cells.

The previous data indicated epithelioid shape was highly indicative of the presence of a CLAN. The decorin-exposed cells exhibited the highest incidence of epithelioid cells with CLANs (79.2%) and the lowest incidence of epithelioid cells with clear prominent stress fibres only (5.9%) whereas DEX was slightly weaker with 70.4% of epithelioid cells containing CLANs and 9.7% with stress fibres but devoid of CLANs. Thus cellular shape of BTM cells may be used as a predictor of CLAN-containing cells.

Imaging reveals divergent shifts in phenotype

A further study was conducted using phase contrast time-lapse imaging to follow the BTM cells for 20 hours after treatment with our CLAN-inducing agents, prior to staining

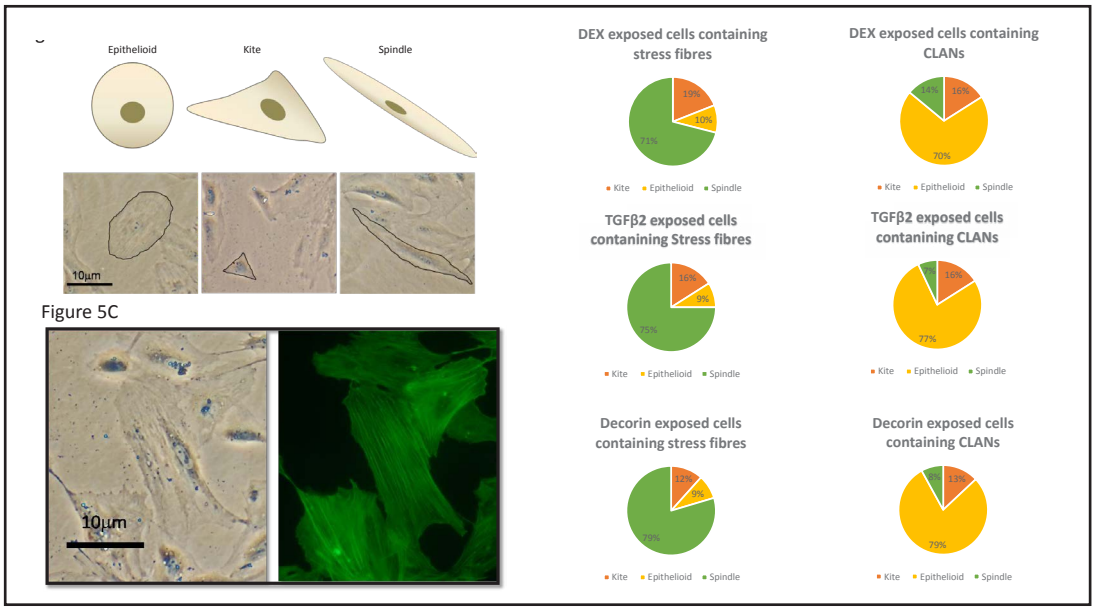

Fig. 5. Variations of cell shape after CLAN induction: A). Idealised images of TM cell shapes cartoon with the phase contrast of the TM cells below. B). Pie charts of TM cell shapes. Pie charts of TM cell shapes which were exposed to the CLAN inducing agents which include DEX, TGF-β2 and decorin and classified as either CLAN-containing or stress fibre-containing cells. N is derived from at least ninety different cells from 3 independent replicates C). Representative phase contrast and F-actin fluorescent image for a BTM cell in vitro with prominent stress fibres contained within the cell.

with phalloidin. Within the filming period most BTM cells maintained their cell shape throughout, however, it was clear that a large proportion of cells altered shape from spindle to epithelioid or epithelioid to spindle. This held for all our CLAN stimulants so arbitrarily we chose to follow the lineages of 100 cells from a DEX treatment experiment. We had traced histories on 55 epithelioid-shaped cell, 31 spindle and 14 kite. Whereas most of the epithelioid appearing BTM cells remained in that form throughout filming (87.3%), the other 2 were less constant with 58.1% spindle cells being without change and hardly any (14.3%) kite-shaped cells. The kite shape appeared to be an intermediate that formed when epithelioid was changing to spindle and vice versa. It was also a form adopted by a mobile BTM cell when it changed direction or came to an abrupt halt. It was apparent in the pre-confluent areas where the cells were more dynamic both in terms of shape-change and clearly in terms of cell movement. It was observed that subsequent to cell division, daughter cells did not contain CLANs or stress fibres.

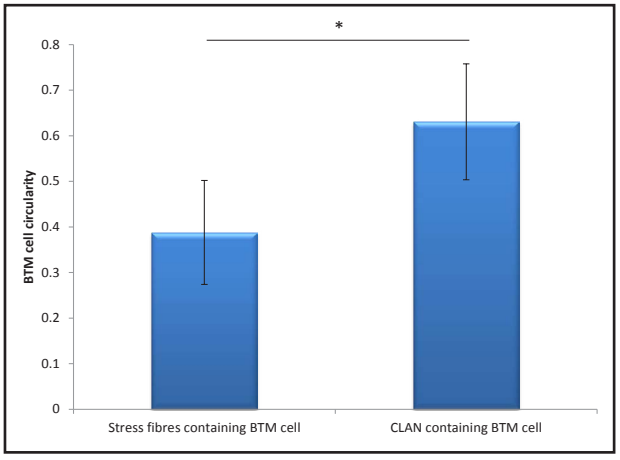

Fig. 6. Comparison of cellular circularity in BTM cells containing either stress fibres or CLANs: Cell circularity was ascertained by image analysis software using the circularity formula as outlined in the methods section with cells containing stress fibres or CLAN actin arrangements. CLAN-containing cells were found to have a significantly higher circularity (*=P=<0.05, Student's t test) ascertained by the circularity equation. Data is mean and SD n=100 cells.

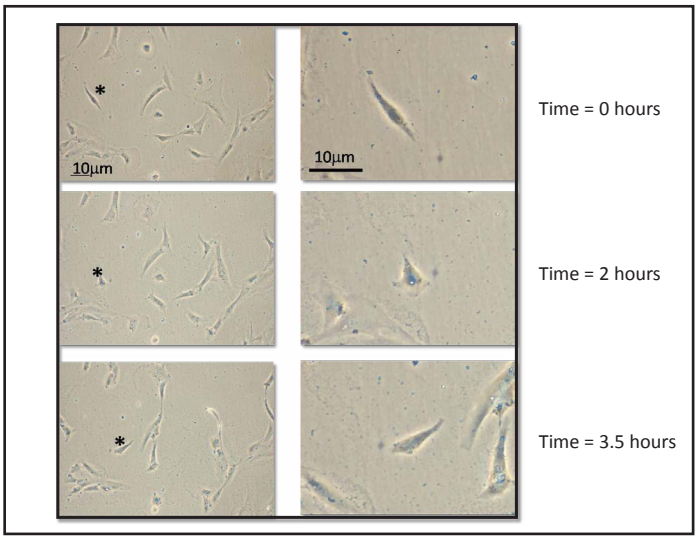

Fig. 7. Time lapse of BTM cells showing shape variation: Phase contrast real time imaging of BTM. Phase contrast time lapse imaging of BTM cell in culture * indicates the BTM cell that was followed as a representative cell over the time period. Scale bar contained within Fig.. t=time.

Regardless of which CLAN-inducing stimulant was used, it was obvious from the time-lapse examination that individual BTM cells showed a wide range of mobility in the pre-confluent parts of the cultures that ranged from stationary (S) to highly mobile (M****). We labelled cells that moved extremely quickly M****, an exceptional event in the cultures, but these rapid cells on phalloidin staining exposed a diffuse actin pattern and never expressed CLANs in their cytoplasm. Analysis of the 100 cell-time-lapse DEX-exposed series started with the phalloidin immunofluorescence and was entirely in line with earlier observations that the CLAN structures were predominantly associated with epithelioid cells and the other pattern of actin arrangement, stress fibers, were restricted to spindle shaped cells. 58.8% of the 51 epithelioid cells containing CLANs that were followed, were classified as being stationary and the rest (41.2%) were mobile, just about (M*). Fig. 7, shows a BTM cell moving in culture through a spindle shape to a kite and back to spindle. Within confluent areas of the culture epithelioid cells would ruffle whereas the spindle shaped cells were more mobile.

Discussion

The TM is a smooth muscle like tissue exhibiting marked contractile properties both *in vitro* and *in vivo* [16-18]. This contractile property is displayed both in human and BTM cells [19].

This cellular contraction is thought to regulate the aqueous humour outflow and thus modulate IOP [17]. Therefore any perturbation of the cellular contractile nature of the tissue would have a profound effect on outflow resistance and hence IOP. Disruption of the actin in TM cells profoundly alters the outflow facility [20, 21] and thus affects IOP and drugs that target this are becoming increasingly attractive. Although in TM cells the stress fibre arrangement of actin predominates, another unusual arrangement of actin occurs termed CLANs. CLANs are geodesic structures found in TM cells both *in vitro*, ex vivo and in situ and are induced by DEX [10] and BTM seem to have a predilection for CLAN formation. However, to date it is unknown whether these strikingly arranged structures had any functional significance.

Here we demonstrated using collagen contraction models that CLANs mediate the inhibition of collagen contraction mainly in the 2D model coincident with CLAN appearance in the TM cells. It may be that in the 3D model of contraction that stress fibre-containing cells predominate, whereas in the 2D model CLAN-containing cells dominate in response to the appropriate stimuli, in this case DEX. It is suggested that these CLANs impart a structural rigidity to the cells that impairs their contractility we had previously found by computer modelling that CLANs affect cell rigidity, rheology and mechanical properties [22]. Analysis of

cell death indicated that this was not significant in this system suggesting that enhanced cell death was not responsible for the reduced contraction of the collagen matrices.

We used a physiological level of 10%/1Hz cyclic mechanical stretch to mimic the pulsatile stretch found *in vivo* and discovered an increase in CLAN levels. Many studies have used mechanical stretch systems using TM cells [23]. Stretch applied for only 12 hours was sufficient to create an increase in CLANs to 40.5% of the cell population. It did not appear that both stimuli DEX and stretch had a synergy in CLAN induction.

With other CLAN inducing agents it can take many days of prolonged exposure for the stimuli to induce appreciable numbers of CLAN however, in this system it has been shown that CLANs are induced after only 12 hours, it may be that the initial biomechanical stimuli is sufficient to muster an early rearrangement of cellular actin.

Some authors reported similar 'CLAN-like' structures in human TM cells subjected to mechanical stretch *in vitro* [17, 24, 25]. Our model of cellular deformation is more physiological and hence more relevant as we used a physiological level of stretch.

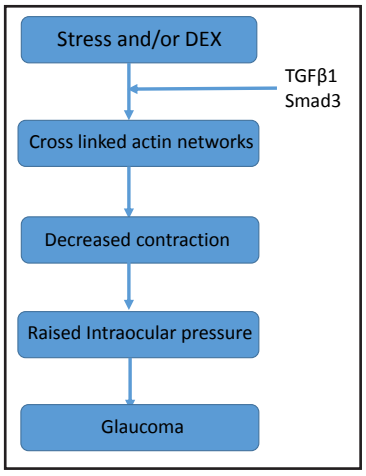

Fig. 8. Possible pathway involving CLAN leading to Glaucoma: Possible pathway of CLAN formation mediated by TGF-β1 signalling which leads to reduced contraction in the TM outflow pathway leading to raised IOP and subsequent POAG.

TGF-β2 is a known inducer of CLANs and is elevated in aqueous humour which bathes the TM in POAG, and we found that stretched cells leads to upregulation of this compared to un-stretched cultures. It could be that stretch-induced increases in TGF-β2 leads to the formation of CLANs, blockade of TGF prior to mechanical stretch induction would be a key experiment to perform to confirm the role of the cytokine in CLAN formation as recent data has suggested that Smads are involved in CLAN formation. Furthermore, it is known that TGF-β1 induces robust upregulation of β3 integrins [26] in cells and this itself could induce CLAN formation.

It was also found that IL-6 was also induced upon stretch and may be influencing cell cytoskeletal arrangement as others have reported [27]. But the significance of this IL-6 increase, if any at all, is unknown. It could be that there is a synergic effect of IL-6 and TGF-β upon the formation of CLANs or indeed an additive effect, however this has to be tested to confirm this suggestion.

We were aware that at least some of the CLAN inducers such as Dex [3], aqueous humour [28] and TGF-β are known to influence cell shape.

As a result, experiments were performed to see if any differences in morphology were discernible in our test BTM cells. Although BTM cells at confluence have been described as being 'endothelial-like' it became apparent that interesting differences in cell appearance and movement particularly during the pre-confluent period. It has been demonstrated that Dex causes shape changes in human endometrial cells and increases TM cell size [29]. TM cells are also known to get more enlarged and rounded in aqueous humour and TGF-β family members also have shape-altering properties promoted by their cytoskeletal modifying effects [30]. What precisely triggers the move to and from a spindle-shaped polarised elongated form to a more circular epithelioid shape and back again is unknown.

Stress fibres were present in all the three shapes of cell seen in BTM cultures i.e. spindle, epithelioid and kite shaped. They were most prominent in the spindle cells but were just as pronounced in stationary spindle cells as they were in the mobile form(s).

Certainly, when TM cells are exposed to the CLAN inducing stimuli we can predict that a rounded, epithelioid stationary cell phenotype has a high probability of having CLANs within the cytoplasm. We now have a shape predictor for the presence of a CLAN, which although not perfect is none the less useful. What is not clear is whether CLANs themselves promote the morphological shape change or whether the shape change precedes CLAN formation?

The ability of the cell to carry out many important cellular functions including replication, phagocytosis, and movement depends on an intact cytoskeleton. The cytoskeleton itself can be highly plastic and respond to external forces and various factors to alter its shape. Recently using porcine TM cells it was shown that CLAN-containing DEX treated cell had reduced migration [31]. The authors also show through live cell imaging with a GFP-actin expression vector that CLANs are both transient and their lifetime increases with the addition of Dex [31]. The authors could not confirm the precise lifetime of CLANs in culture but suggest that they could be extremely long-lived structures. The association with reduction of movement is consistent with our findings and our previous modelling suggesting alterations in compression forces and it is known that the glaucomatous TM is stiffer [32]. Key questions about the life-time of CLANs remain and technical limitations do hamper the tracing of such structures in real time.

Conclusion

We show a functional effect of CLANs in TM cells and that a physiologically relevant mechanical stretch promotes CLAN formation *in vitro*. This could have implications on the pathogenesis of POAG where there is clear disruption to the flow of aqueous humour. The fact that TGF-β2 is elevated in POAG and mediates CLANs suggests this molecule warrants further investigation into a possible pathway (Fig. 8). Furthermore, we demonstrate that CLAN-containing cells can be phenotypically identified based on simple light microscopy. Further work is required to determine if this is relevant using human TM cells.

Acknowledgements

LD and SOR performed experiments and wrote manuscript.

Disclosure Statement

The authors can confirm that they have nothing to disclose.

References

1 Pellegrin S, Mellor H: Actin stress fibres. J Cell Sci 2007;120:3491-3499.
2 Lazarides E: Actin, alpha-actinin, and tropomyosin interaction in the structural organization of actin filaments in nonmuscle cells. J Cell Biol 1976;68:202-219.
3 Clark AF, Wilson K, McCartney MD, Miggans ST, Kunkle M, Howe W: Glucocorticoid-induced formation of cross-linked actin networks in cultured human trabecular meshwork cells. Invest Ophthalmol Vis Sci 1994;35:281-294.
4 Clark AF, Brotchie D, Read AT, Hellberg P, English-Wright S, Pang IH, Ethier CR, Grierson I: Dexamethasone alters F-actin architecture and promotes cross-linked actin network formation in human trabecular meshwork tissue. Cytoskeleton 2005;60:83-95.
5 Clark AF, Miggans ST, Wilson K, Browder S, McCartney MD: Cytoskeletal changes in cultured human glaucoma trabecular meshwork cells. J Glaucoma 1995;4:183-188.
6 Ireland G, Voon F: Polygonal networks in living chick embryonic cells. J Cell Sci 1981;52:55-69.
7 Mochizuki Y, Furukawa K, Mitaka T, Yokoi T, Kodama T: Polygonal networks,"geodomes", of adult rat hepatocytes in primary culture. Cell Biol Int Rep 1988;12:1-7.
8 Meller K, Theiss C: Atomic force microscopy and confocal laser scanning microscopy on the cytoskeleton of permeabilised and embedded cells. Ultramicroscopy 2006;106:320-325.
9 Ingber DE: Cellular mechanotransduction: putting all the pieces together again. FASEB J 2006;20:811-827.
10 Wade N, Grierson I, O'reilly S, Hoare M, Cracknell K, Paraoan L, Brotchie D, Clark A: Cross-linked actin networks (CLANs) in bovine trabecular meshwork cells. Exp Eye Res 2009;89:648-659.

11 Bell E, Ivarsson B, Merrill C: Production of a tissue-like structure by contraction of collagen lattices by human fibroblasts of different proliferative potential *in vitro*. Proc Natl Acad Sci U S A 1979;76:1274-1278.
12 Coleman DJ, Trokel S: Direct-recorded intraocular pressure variations in a human subject. Arch Ophthalmol 1969;82:637-640.
13 Johnstone MA: The aqueous outflow system as a mechanical pump: evidence from examination of tissue and aqueous movement in human and non-human primates. J Glaucoma 2004;13:421-438.
14 Filla MS, Woods A, Kaufman PL, Peters DM: β1 and β3 integrins cooperate to induce syndecan-4-containing cross-linked actin networks in human trabecular meshwork cells. Invest Ophthalmol Vis Sci 2006;47:1956-1967.
15 Standley PR, Camaratta A, Nolan BP, Purgason CT, Stanley MA: Cyclic stretch induces vascular smooth muscle cell alignment via NO signaling. Am J Physiol Heart Circ Physiol 2002;283:H1907-H1914.
16 Lepple-Wienhues A, Stahl F, Wiederholt M: Differential smooth muscle-like contractile properties of trabecular meshwork and ciliary muscle. Exp Eye Res 1991;53:33-38.
17 Wiederholt M, Thieme H, Stumpff F: The regulation of trabecular meshwork and ciliary muscle contractility. Prog Retin Eye Res 2000;19:271-295.
18 Rosenthal R, Choritz L, Schlott S, Bechrakis NE, Jaroszewski J, Wiederholt M, Thieme H: Effects of ML-7 and Y-27632 on carbachol-and endothelin-1-induced contraction of bovine trabecular meshwork. Exp Eye Res 2005;80:837-845.
19 Thieme H, Hildebrandt J, Choritz L, Strauss O, Wiederholt M: Muscarinic receptors of the M2 subtype in human and bovine trabecular meshwork. Graefes Arch Clin Exp Ophthalmol 2001;239:310-315.
20 Johnson DH, Tschumper RC: Ethacrynic acid: outflow effects and toxicity in human trabecular meshwork in perfusion organ culture. Curr Eye Res 1993;12:385-396.
21 Cai S, Liu X, Glasser A, Volberg T, Filla M, Geiger B, Polansky JR, Kaufman PL: Effect of latrunculin-A on morphology and actin-associated adhesions of cultured human trabecular meshwork cells. Mol Vis 2000;6:132-143.
22 Zheng Y, Currie L, Pollock N, Heath A, Sheridan C, Choudhary A, O'Reilly S, Grierson I: Measurement and Computer Modeling of Temporary Arrangements of Polygonal Actin Structures in Trabecular Meshwork Cells Which Consist of Cross-Linked Actin Networks and Polygonal Actin Arrangements. J Ocul Pharmacol Ther 2014;30:224-236.
23 Bradley JM, Kelley MJ, Zhu X, Anderssohn AM, Alexander JP, Acott TS: Effects of mechanical stretching on trabecular matrix metalloproteinases. Invest Ophthalmol Vis Sci 2001;42:1505-1513.
24 Tumminia SJ, Mitton KP, Arora J, Zelenka P, Epstein DL, Russell P: Mechanical stretch alters the actin cytoskeletal network and signal transduction in human trabecular meshwork cells. Invest Ophthalmol Vis Sci 1998;39:1361-1371.
25 Grierson I, Lee WR, Abraham S: Effects of pilocarpine on the morphology of the human outflow apparatus. Br J Ophthalmol 1978;62:302-313.
26 Pechkovsky DV, Scaffidi AK, Hackett TL, Ballard J, Shaheen F, Thompson PJ, Thannickal VJ, Knight DA: Transforming Growth Factor 1 Induces v 3 Integrin Expression in Human Lung Fibroblasts via a 3 Integrin-, c-Src-, and p38 MAPK-dependent Pathway. J Biol Chem 2008;2008:12898-12908.
27 Zhongbiao W, Walter HN: Smooth muscle cell migration stimulated by interleukin 6 is associated with cytoskeletal reorganization. J Surg Res 2003;111:261-266.
28 Fautsch MP, Howell KG, Vrabel AM, Charlesworth MC, Muddiman DC, Johnson DH: Primary trabecular meshwork cells incubated in human aqueous humor differ from cells incubated in serum supplements. Invest Ophthalmol Vis Sci 2005;46:2848-2856.
29 Wilson K, McCartney MD, Miggans ST, Clark AF: Dexamethasone induced ultrastructural changes in cultured human trabecular meshwork cells. Curr Eye Res 1993;12:783-793.
30 Nakamura Y, Hirano S, Suzuki K, Seki K, Sagara T, Nishida T: Signaling Mechanism of TGF-β1–Induced Collagen Contraction Mediated by Bovine Trabecular Meshwork Cells. Invest Ophthalmol Vis Sci 2002;43:3465-3472.
31 Fujimoto T, Inoue T, Inoue-Mochita M, Tanihara H: Live cell imaging of actin dynamics in dexamethasone-treated porcine trabecular meshwork cells. Exp Eye Res 2016;145:393-400.
32 Last JA, Pan T, Ding Y, Reilly CM, Keller K, Acott TS, Fautsch MP, Murphy CJ, Russell P: Elastic modulus determination of normal and glaucomatous human trabecular meshwork. Invest Ophthalmol Vis Sci 2011;52:2147-2152.